The influence of weak attractive forces on the microstructure and rheology of colloidal dispersions

Lakshmi-narasimhan Krishnamurthy and Norman J. Wagner[a)]

Center for Molecular and Engineering Thermodynamics, Department of Chemical Engineering, University of Delaware, Newark, Delaware 19716

(Received 23 July 2004; final revision received 17 December 2004)

Synopsis

Rheology is demonstrated to be a sensitive and quantitative probe of weak attractive forces acting in concentrated stable colloidal dispersions through comparison of rheology and small-angle neutron scattering measurements on a model dispersion with added polyampholyte. Polyampholyte-stabilized dispersions are found to exhibit weak attractions in the form of depletion forces arising from free polyampholyte in the suspending medium. The depletion potential is modeled with the Asakura-Oosawa potential and mapped onto the sticky hard sphere potential to facilitate modeling. Independent validation of the interparticle potential is provided by quantitative prediction of the measured small-angle neutron scattering spectra. A new semiempirical predictive model for the low shear viscosity of stable dispersions is proposed and validated against measurements on model dispersions over a range of compositions. This rheological constitutive relation provides an improved prediction of the low shear viscosity of stable mixtures of adsorbing polyampholyte and colloidal particles, and is anticipated to have broad applicability in modeling and predicting colloidal suspension viscosity. © *2005 The Society of Rheology.* [DOI: 10.1122/1.1859792]

I. INTRODUCTION

Colloidal particles are incorporated into a wide range of industries and products. A thorough understanding of dispersion rheology and stability is beneficial for successful formulation and processing of colloidal dispersions for practical applications [Hiemenz and Rajagopalan (1997); Howe (2000)]. Of particular interest in this work are dispersions relevant to the photographic industry, where the degree of dispersion directly impacts the image quality, and the dispersion rheology and stability under high deformation rates is crucial to successful coating processing. Although the focus of this work is to predict the dispersion rheology of colloidal dispersions stabilized by polyampholytes (gelatin), the methodology presented here has direct applicability to a broad class of polymer-stabilized colloidal dispersions.

The rheology and stability of colloidal dispersions are direct reflections of the potential of interaction acting between the colloids [Russel *et al.* (1989)]. The interparticle forces arising from the addition of polymers include bridging and steric forces due to adsorption, depletion forces from the dissolved polymer, as well as an electrosteric force if the polymer is charged [Asakura and Oosawa (1958); Brady (1993); Buscall *et al.*

[a)]Author to whom correspondence should be addressed; electronic mail: wagner@che.udel.edu

(1993); Hiemenz and Rajagopalan (1997); Likos *et al.* (2000); Fritz *et al.* (2002)]. Adsorption of polymers on colloidal surfaces in good to theta solvents provides a steric repulsion between the adsorbed brushes, which imparts colloidal stability. The presence of free polymer generates an attractive force due to depletion effects that can lead to gelation or crystallization [Gast *et al.* (1983)].

In this work, we investigate the influence of gelatin, an amphoteric biopolymer, on the rheology and liquid phase microstructure of model colloid dispersions with the goal of quantitatively connecting the interparticle forces to the dispersion properties. The stabilizing effect of gelatin adsorption onto different substrates, both flat and colloidal, has been studied extensively in the literature [Kamiyama and Israelachvili (1992); Vaynberg *et al.* (1998); Hone *et al.* (2000); Likos *et al.* (2000); Eck *et al.* (2001); Vaynberg and Wagner (2001); Hone and Howe (2002); Krishnamurthy *et al.* (2004)]. Under conditions of like net charge on the particles and polyampholyte, the rheology of gelatin-stabilized dispersions is dominated by the excluded volume interactions arising from gelatin adsorption [Vaynberg and Wagner (2001)], which is similar to other steric-stabilized dispersions [Mewis and Vermant (2000)]. In recent work [Krishnamurthy *et al.* (2004)], it has been shown that the zero-shear viscosities of stable aqueous colloidal dispersions with added gelatin are predictable using an effective osmotic overlap potential accounting for the adsorption of gelatin onto the particles. However, systematic deviations from the model predictions and qualitative differences in rheology upon the addition of substantial amounts of excess gelatin [Hone and Howe (2002)] remain unexplained.

In addition, there are discrepancies with potential parameters deduced from small-angle neutron scattering (SANS) measurements on gelatin-stabilized dispersions [Cosgrove *et al.* (1998); Likos *et al.* (2000)]. It was observed that the adsorbed layer was significantly thinner than that determined from dynamic light scattering (DLS) or deduced from rheology. The hydrodynamic size of the gelatin-colloid complex determined from DLS is found to be comparable, but systematically lower, than the size calculated from rheology. The interparticle potentials used in these previous studies were purely repulsive potentials arising from steric interactions of the adsorbed layer and electrostatic repulsions from the net particle charge. It will be shown here that this framework is inadequate for describing colloid dispersions in the presence of adsorbing polyampholyte. Rather, accounting for additional weak interparticle attractions arising from the free polyampholyte can reconcile the observed rheological and neutron scattering data.

An idealized stable mixture of colloids and adsorbing polymer at equilibrium should not exhibit a depletion attraction due to the free polymer in solution if the free and adsorbed polymer are in equilibrium. However, it has been shown through measurements of phase behavior [Snowden *et al.* (1991); Smith and Williams (1995)] that the unabsorbed polymer fraction in a polymer-colloid mixture can induce a depletion attraction even when the polymer adsorbs. This was attributed to the nonequilibrium nature of polymer adsorption. Previous studies on gelatin-stabilized dispersions have not considered depletion interactions arising from free gelatin.

Weak interparticle attractions are expected to increase the viscosity of colloidal solutions as shown theoretically for a dilute square-well fluid [Bergenholtz and Wagner (1994)] and for a dilute sticky hard sphere fluid [Russel (1984); Cichocki and Felderhof (1990); Baxter (1968)]. Experiments [Woutersen and De Kruif (1991); Buscall *et al.* (1993); Rueb and Zukoski (1998)] at high colloid concentrations have shown that colloidal attractions increase the low shear rate viscosity. Empirical modeling of experimental data by Buscall *et al.* (1993) shows that a linear increase in the strength of the attractive interactions results in an exponential increase in viscosity. These existing theories and

TABLE I. Material properties.

	Batch	Diameter (nm)	surface potential (mV)	Concentration	IEP	Mn (Da)	Density (g/cc)
Silica	30V25 provided by Clariant Inc.	31 (DLS)	−29	30 wt %	2	⋯	2.2
Gelatin	Gel-37 provided by Eastman Kodak Company	28[a] (SANS)		⋯	4.9	100 000	1.3

[a] $R_g = 14 \pm 2$ from Vaynberg *et al.* (1998).

models for the rheology of colloidal systems with weak attractions provide guidance in developing a predictive model for polyampholyte-colloid dispersions.

Although the specific goal of this research is to develop a predictive model for the rheology and stability of colloidal dispersions in the presence of gelatin, the underlying modeling is expected to have a much broader applicability. The route to achieving this is through a model for the interparticle potential, which can be used within the framework of statistical mechanics to calculate the suspension microstructure and rheology. It has been shown in our previous work [Krishnamurthy *et al.* (2004)] that an osmotic overlap potential can be used to semiquantitatively predict the rheology of gelatin-colloid mixtures. Here, we extend this formalism by incorporating the osmotic depletion interaction of free polymer using the model of [Asakura and Oosawa (1954, 1958)]. We propose a new predictive model for the zero-shear viscosity of dispersions with weak attractive interactions applicable over the entire concentration range. Validation is shown through quantitative comparison of rheology and SANS measurements.

II. EXPERIMENTAL

Colloidal silica nanoparticles, obtained from Clariant Inc., and lime processed deionized gelatin from Eastman Kodak, were used in this work. The samples and experiments have been described more extensively in previous work [Krishnamurthy *et al.* (2004)]. The relevant properties of the samples are provided in Table I. In preparing the samples, gelatin was soaked in sodium acetate (NaAc) buffer for 1 h at room temperature and then gently stirred into a homogeneous solution at 40 °C for 1 h to obtain a 10 wt % gelatin stock solution. As the majority of experiments were performed in 0.01 M NaAc buffer, the silica dispersion as received was dialyzed against a bath containing 0.01 M NaAc to control the *p*H at 8.0 and ionic strength at 10 mM prior to preparation of the gelatin-silica mixtures. The resultant stock particle dispersion contained 30.33 wt % silica. Silica-gelatin mixtures were prepared by diluting the stock particle solution with NaAc buffer and then adding the required amount of gelatin stock solution to obtain the desired final composition. The concentrations of the components in the aqueous phase are reported on a silica-free basis. All mixtures were incubated at 40 °C for 16 h prior to experimentation.

Rheological studies were performed on a Rheometric Scientific stress-controlled rheometer (SR-5000) equipped with a couette cell (17 mm outer diameter and 16.5 mm inner diameter) at 40 ± 0.1 °C. Samples were enclosed in a low viscosity mineral oil to avoid drying according to a protocol previously discussed [Vaynberg and Wagner (2001)]. The rheological protocol consisted of descending and ascending stress sweeps in series. All reported viscosities are time independent, reproducible, and independent of

tool geometry. Dynamic oscillatory measurements demonstrated no measurable elasticity and there was no evidence of slip or yielding for any of the samples.

Intrinsic viscosity measurements for gelatin and the gelatin-colloid complexes were performed using a calibrated Canon-Ubbelohde viscometer (N31 and L62) at 40 ± 0.1 °C. The density of these solutions was measured using an Anton-Paar densitometer (DMA 35) to extract the shear viscosity from the capillary measurements of kinematic viscosity.

SANS measurements were performed on the samples at the NG3 SANS line at National Institute of Standards and Technology (NIST). Samples were held at 40 ± 0.1 °C in 1 mm cells. Thermal neutrons of 6 Å and 14.7% half-width dispersity were used at detector distances of 3.8 m and 13 m. The measured scattering intensities were reduced to the absolute scale using the standard NIST procedure.

III. THEORY

A. Zero-shear viscosity of near-hard sphere dispersions with weak attractions

The starting point for the theoretical development of a model for the rheology of weakly attractive colloidal systems is that of hard-sphere dispersions. Einstein derived the exact dilute limiting form for the relative viscosity ($\eta_{r0} = \eta_{\text{suspension}}/\eta_{\text{medium}}$) that was extended by Batchelor [Batchelor (1977, 1983)] to include interparticle interactions. The expansion written in terms of volume fraction of colloids is

$$\eta_{r0} = 1 + ([\eta]\rho)\phi + k_H([\eta]\rho)^2\phi^2. \tag{1}$$

This expression is valid until volume fractions of $\phi \sim 0.1$. In the above, ρ is the particle density, $[\eta]$ is the intrinsic viscosity of the particles and k_H the Huggins coefficient. $[\eta]$ was calculated by Einstein (1906) to be $2.5/\rho$ and k_H was calculated to be 0.946 [Bergenholtz and Wagner (1994)] for Brownian hard-sphere dispersions.

At higher concentrations, no exact theoretical models exist for even simple hard spheres. To within a reasonable degree of accuracy, phenomenological models of Krieger and Dougherty (1959) and Quemada (1977), both of which incorporate one parameter, the maximum packing fraction ($\phi_{\max}$), have been shown to be reasonable approximations of the relative zero shear of hard-sphere dispersions [$\eta_{r0}^{\text{HS}}(\phi)$]. In this study, we employ the following relation:

$$\eta_{r0}^{\text{HS}}(\phi) = \left(1 - \frac{\phi}{\phi_{\max}}\right)^{-2}. \tag{2}$$

An alternate model based on the empirical Dolittle equation has been correlated to the zero-shear viscosity measurements on model hard-sphere dispersions [Cheng *et al.* (2002)]:

$$\eta_{r0}^{\text{HS}}(\phi) = \eta'_{r\infty}\left(1 + 0.225 \exp - \left(\frac{0.9\phi\phi_{\max}}{\phi_{\max} - \phi}\right)\right), \tag{3}$$

where $\eta'_{r\infty}$ is the relative high-frequency viscosity of a hard sphere dispersion given by:

$$\eta'_{r\infty} = \frac{\eta'_{\infty}}{\eta_{\text{medium}}} = \frac{1 + \frac{3}{2}\phi[1 + \phi(1 + \phi - 2.3\phi^2)]}{1 - \phi[1 + \phi(1 + \phi - 2.3\phi^2)]}. \tag{4}$$

Finally, we note that micromechanical models with various degrees of approximation for many body thermodynamic and hydrodynamic interactions have been proposed and

tested against data for the zero-shear viscosity of hard sphere dispersions, as well as simulations [Brady (1993); Lionberger and Russel (2000)].

Various authors [Russel (1984); Cichocki and Felderhof (1990); Buscall *et al.* (1993)] have extended the theories for hard-sphere dispersions to colloidal dispersions with weak attractions. Russel (1984) has proposed an exact theory for viscosity of systems with weak attraction at low colloid densities. The attractive part of the potential is characterized by τ_b, the "sticky parameter" for the Baxter potential [Baxter (1968)]. The presence of weak attractions does not affect the intrinsic viscosity, but modifies the Huggins coefficient. Cichocki and Felderhof (1990) numerically calculated the correction to the ϕ^2 term in the viscosity expansion to be

$$\eta_{r0} = 1 + 2.5\phi + \left(5.9 + \frac{1.9}{\tau_b}\right)\phi^2. \tag{5}$$

Equation (5) is exact for dilute dispersions of Brownian hard spheres interacting via the sticky hard-sphere potential. However, it can be used to describe more realistic potentials through equating the second virial coefficients to determine τ_b [Rueb and Zukoski (1998)]. Extensive numerical results also exist for the ϕ^2 coefficient for particles interacting with the square-well potential [Bergenholtz and Wagner (1994)].

At higher colloidal concentrations, semiempirical corrections to the hard-sphere equations have been proposed. Buscall *et al.* (1993) fit data for low shear viscosity of a colloidal dispersion with a nonadsorbing polymer to a phenomenological equation of the form:

$$\eta_{r0} = K \exp\left(-\frac{\alpha(\phi,a)U_0}{kT}\right). \tag{6}$$

The minimum in the interparticle potential U_0 was estimated from independent measurements of free polymer properties. The parameter $\alpha(\phi,a)$ was fit to the data and was expected to depend on volume fraction and particle size. In the manuscript, it was suggested that the term K should be the relative viscosity of a hard-sphere system. The experimental data validated the exponential dependence on well depth.

To date, there are no *predictive* theories for the low shear viscosity valid over the entire range of volume fractions for colloidal dispersions with attractive interactions. Here, we develop a semiempirical predictive model by matching the exact dilute limiting expansion Eq. (5) to a dilute limiting expansion of the phenomenological model of Buscall *et al.* [Eq. (6)], thereby deriving the parameter $\alpha(\phi,a)$. The exponential of the well depth can be related to the last term in Eq. (5) as follows. Defining K to be η_{r0}^{HS} for hard-sphere dispersion and expanding Eq. (6) for low volume fractions yields:

$$\eta_{r0}|_{\phi\to 0} = (1 + 2.5\phi + 5.9\phi^2)\exp\left(\frac{\alpha(-U_0)}{kT}\right). \tag{7}$$

Comparing this to Eq. (5) yields (correct to the order ϕ^2 terms):

$$\lim_{\phi\to 0} \exp\left(-\frac{\alpha U_0}{kT}\right) \Rightarrow 1 + \frac{1.9\phi^2}{\tau_b}. \tag{8}$$

This result is not surprising as the sticky parameter τ_b is also related to the exponential of the well depth in typical mappings used to analyze the scattering, which will be shown shortly. Then, the predictive semiempirical equation for the zero-shear viscosity of colloidal dispersion with weak attractive interaction becomes

$$\eta_{r0} = \eta_{r0}^{\mathrm{HS}}(\phi)\left(1 + \frac{1.9\phi^2}{\tau_b}\right). \tag{9}$$

For use at higher packing fractions, various models for the hard-sphere viscosity are available, such as that given by Eq. (2), which requires an additional parameter, the maximum packing fraction $\phi_{\max}$. For the dispersions under consideration here which have a long-range attractive interaction (relative to the particle size), the value of $\phi_{\max} = 0.58$, as predicted from mode coupling calculations of the colloidal glass transition in square-well dispersion by Dawson *et al.* (2001) for wide well widths.

The value of τ_b can be calculated for a given potential $U(r)$ by matching the second virial coefficients $B_2(T)$, defined generally as [Russel *et al.* (1989); McQuarrie (2000)]:

$$B_2(T) = 2\pi \int_0^\infty (1 - e^{-U(r)/kT}) r^2 dr \tag{10}$$

For the Baxter sticky hard-sphere potential [Russel (1984); Menon *et al.* (1991)], this becomes

$$\frac{B_2(T)}{B_2^{\mathrm{HS}}} = 1 - \frac{1}{4\tau_b}. \tag{11}$$

For modeling SANS spectra, we employ a square-well potential. For a square well of depth U_0 and width Δ, the second virial coefficient is [Menon *et al.* (1991)]

$$\frac{B_2(T)}{B_2^{\mathrm{HS}}} = 1 - (e^{-U_0/kT} - 1)\left(\left(\frac{\sigma + \Delta}{\sigma}\right)^3 - 1\right) \tag{12}$$

In the above, $B_2^{\mathrm{HS}} = 2\pi\sigma^3/3$ is the second virial coefficient for hard spheres [McQuarrie (2000)].

B. Small-angle neutron scattering

The intensity of coherently scattered neutrons $I(q)$ for a system of monodisperse spheres is [Hansen and McDonald (1986); McQuarrie (2000)]

$$I(q) = \phi V_p \Delta\rho_s^2 P(q) S(q), \tag{13}$$

where V_p is the volume of a particle, $\Delta\rho_s$ is the difference in scattering length densities between the colloid and the medium, $P(q)$ is the form factor of a single scatterer, $S(q)$ accounts for the interparticle structure, and $q = 4\pi/\lambda_n \sin(\theta/2)$ is the magnitude of the scattering vector. The terms $(\phi V_p \Delta\rho_s^2)$ can be grouped into a single prefactor I_0.

The form factor $P(q)$ gives information on the shape and size of a single scatter, while the structure factor $S(q)$ is the Fourier transform of the pair distribution function $g(r)$ and depends on the interaction potential. Thus, SANS provides another sensitive probe of the interparticle interactions.

The form factor of a homogeneous sphere of radius $\sigma/2$ is given by

$$P(q) = f(q)^2 = \left[\frac{3(\sin(q\sigma/2) - q\sigma/2\cos(q\sigma/2))}{(q\sigma/2)^3}\right]^2. \tag{14}$$

Figure 1(a) shows the fit of this form factor corrected for instrument smearing and polydispersity to measurements on colloidal silica dispersions (155 nm radius and 8% polydispersity) in D_2O at a low concentration. Figure 1(b) shows the predicted form factor of the silica particles dispersed in 5 mg/ml gelatin in aqueous buffer assuming the

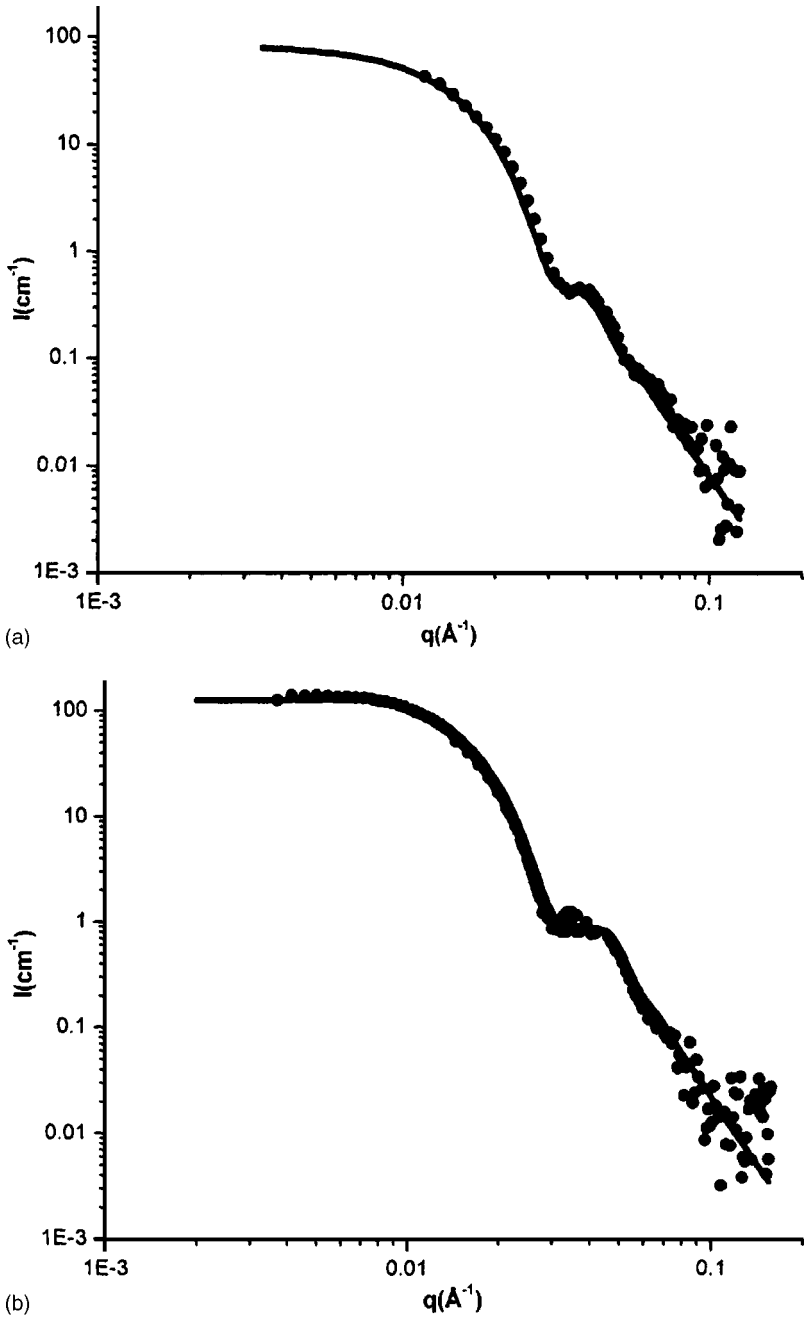

FIG. 1. (a) Form factor: Comparison of measured form factor with the calculated value Eq. (14) for silica in D_2O. (b) Form factor: Comparison of measured form factor with the calculated value Eq. (14) assuming the scattering is from the silica particles. $\phi_{\text{silica}}=0.009$, $T=40\ ^\circ\text{C}$, and gelatin is 5 mg/ml.

scattering is only from the silica particles and using with the same parameters as those in Fig. 1(a), compared against measurements. The constant I_0 for scattering has been calculated using the reported values of scattering length densities [Pezron *et al.* (1991); Cosgrove *et al.* (1998); Likos *et al.* (2000)] given in Table II. The calculated and best-fit

TABLE II. Scattering length densities of individual components.

	ρ_s (Å^{-2})
Gelatin	3.67*E*−07
Water	−5.60*E*−07
Silica	3.47*E*−06

values are in good quantitative agreement and are within the uncertainty in the reported and calculated parameters. Therefore, it can be concluded that the dominant contribution to the SANS comes from the silica particles in aqueous mixtures of silica with gelatin; i.e., under the conditions here, the adsorbed gelatin is essentially transparent to the neutrons. This result is consistent with the magnitudes of the scattering length densities and solution concentrations, and simplifies the analysis of SANS from more concentrated solutions.

The potential of interaction is related to the pair density distribution function through the Ornstein-Zernike equation [Hansen and McDonald (1986); McQuarrie (2000)]

$$h(r) = c(r) + \rho \int c(\mathbf{r} - \mathbf{r}')h(\mathbf{r}')d\mathbf{r}, \tag{15}$$

where $h(r)=g(r)-1$ is the total correlation function and $c(r)$ is the direct correlation function. The Percus-Yevick relation is used to close this equation connecting $c(r)$ to $g(r)$ and the pair potential

$$c(r) = g(r)\left(1 - \exp\left(\frac{U(r)}{kT}\right)\right). \tag{16}$$

Thus, given the potential of interaction $U(r)$, Eqs. (15) and (16) can be used to determine the pair density distribution function $g(r)$, which is the Fourier transform of the structure factor $S(q)$

$$S(q) = 1 + \rho \int e^{-i\mathbf{q}\cdot\mathbf{r}}(g(r) - 1)d\mathbf{r}. \tag{17}$$

The above equations are used to predict structure factors for hard-sphere dispersions. For modeling, the effect of an attractive square-well interaction, a perturbation solution proposed by Menon *et al.* (1991), is employed. These structure factors are a function of the square-well depth U_0 and well width Δ, valid for $\Delta/\sigma < 5\%$,

$$S(q) = \frac{1}{A^2(q) + B^2(q)}, \tag{18}$$

where

$$A(q) = 1 + 12\omega\left\{\alpha\left[\frac{\sin(q) - q\cos(q)}{q^3}\right] + \beta\left[\frac{1 - \cos(q)}{q^2}\right] - \frac{\lambda}{12}\frac{\sin(q)}{q}\right\}, \tag{19}$$

$$\text{and } B(q) = 12\omega\left\{\alpha\left[\frac{1}{2q} - \frac{\sin(q)}{q^2} + \frac{1-\cos(q)}{q^3}\right] + \beta\left[\frac{1}{q} - \frac{\sin(q)}{q^2}\right] - \frac{\lambda}{12}\left[\frac{1-\cos(q)}{q}\right]\right\}. \tag{20}$$

The parameters α, β, and λ are determined from the potential parameters and colloid diameter σ volume fraction ϕ. In the above, λ is the solution to the quadratic equation

$$\lambda\tau = \frac{\left(1+\frac{\omega}{2}\right)}{(1-\omega)^2} - \frac{\lambda\omega}{(1-\omega)} + \frac{\lambda^2\omega}{12}, \tag{21}$$

where

$$\omega = \phi\left\{\sigma\left(1+\frac{\Delta}{\sigma}\right)\right\}^3, \tag{22}$$

and

$$\tau = \frac{1}{12\left(\frac{\Delta}{\sigma}\right)} e^{U_0/kT}. \tag{23}$$

The other two functions in the structure factor can then be calculated from

$$\alpha = \frac{1+2\omega-\lambda\omega(1-\omega)}{(1-\omega)^2}, \tag{24}$$

and

$$\beta = \frac{-3\omega+\lambda\omega(1-\omega)}{2(1-\omega)^2}. \tag{25}$$

The corrections to the structure factor for particle size paucidispersity $[S_{\text{polydis}}(q)]$ were made according the procedure described by Kotlarchyk and Chen (1983).

$$S_{\text{polydis}}(q) = 1 + \frac{|\langle f(q)\rangle|^2}{\langle|f(q)|^2\rangle}(S(q)-1). \tag{26}$$

Finally, the calculated scattering intensity for dispersions of polydisperse spheres are also corrected for the instrument smearing by convoluting with a normal distribution $N(q-q_0)$, the width of which is given by the full width at half maximum (FWHM) of the incident neutrons as shown in

$$I(q_0) = \int I_0 P(q) S_{\text{polydis}}(q) N(q-q_0) dq. \tag{27}$$

This "smeared" intensity can be compared directly with the measured intensity.

C. Potential of interaction

In this work, we hypothesize that the free unabsorbed gelatin leads to a depletion attraction. Asakura and Oosawa (1954, 1958) proposed the depletion potential for dilute colloidal spheres dispersed in an idealized polymer solution. The total potential is a sum of the electrosteric repulsion due to adsorbed polyampholyte [Krishnamurthy *et al.* (2004)], which is modeled as an osmotic overlap potential, and the Asakura-Oosawa

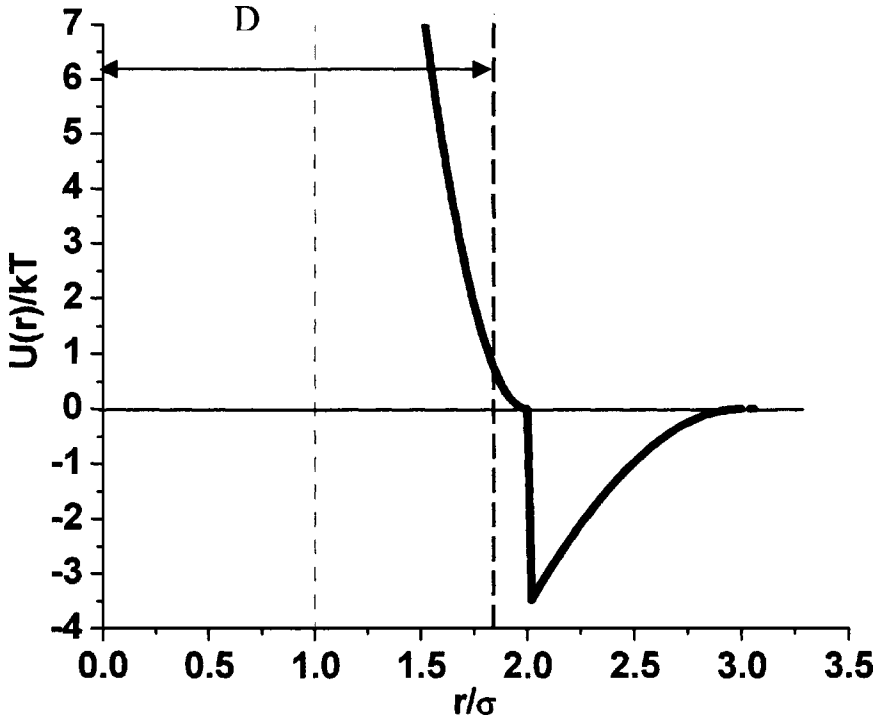

FIG. 2. Osmotic potential with $\sigma = 31$ nm, $L = 15.5$ nm, $\Pi_{\text{gelatin}} = 5000$ Pa, attractive $\Pi_{\text{gelatin}} = 450$ Pa and $R_g = 15$ nm. It is assumed that the adsorbed layer is incompressible, hence the potential diverges at $r = 1.5\ \sigma$.

potential for depletion arising from the unabsorbed, or "free" gelatin. The functional form of this potential for two colloids with diameter σ interacting with adsorbed polymer of layer thickness L and a free polymer of radius of gyration R_g providing the depletion, at a center-to-center separation distance r is

$$U(r) = \begin{cases} \infty & r < \sigma + L \\ \Pi_{\text{gelatin}}^{\text{overlap}} V_{\text{overlap}} & \sigma + L < r < \sigma + 2L \\ -\Pi_{\text{gelatin}}^{\text{free}} V_{\text{depletion}} & \sigma + 2L < r < \sigma + 2L + 2R_g \\ 0 & r > \sigma + 2L + 2R_g, \end{cases} \tag{28}$$

where $\Pi_{\text{gelatin}}^{\text{overlap}}$ is the osmotic pressure of gelatin in the overlap layer contributing to repulsion and $\Pi_{\text{gelatin}}^{\text{free}}$ is the osmotic pressure of free gelatin providing the attraction. The volume of the overlap layer V_{overlap} is given by $V_{\text{overlap}} = \pi\sigma(L - H/2)^2$ and the volume of the depletion layer $V_{\text{depletion}}$ is given by

$$V_{\text{depletion}} = \frac{4\pi R_g^3}{3}\left(1 - \frac{3r}{2\left(\frac{\sigma}{2} + R_g\right)} + \frac{r^3}{16\left(\frac{\sigma}{2} + R_g\right)^3}\right). \tag{29}$$

The form of the potential is shown in Fig. 2. The repulsive part of the potential can be further modeled using Barker Henderson perturbation theory to map onto an effective hard-sphere dispersion with diameter D [Barker and Henderson (1967a, b)], yielding:

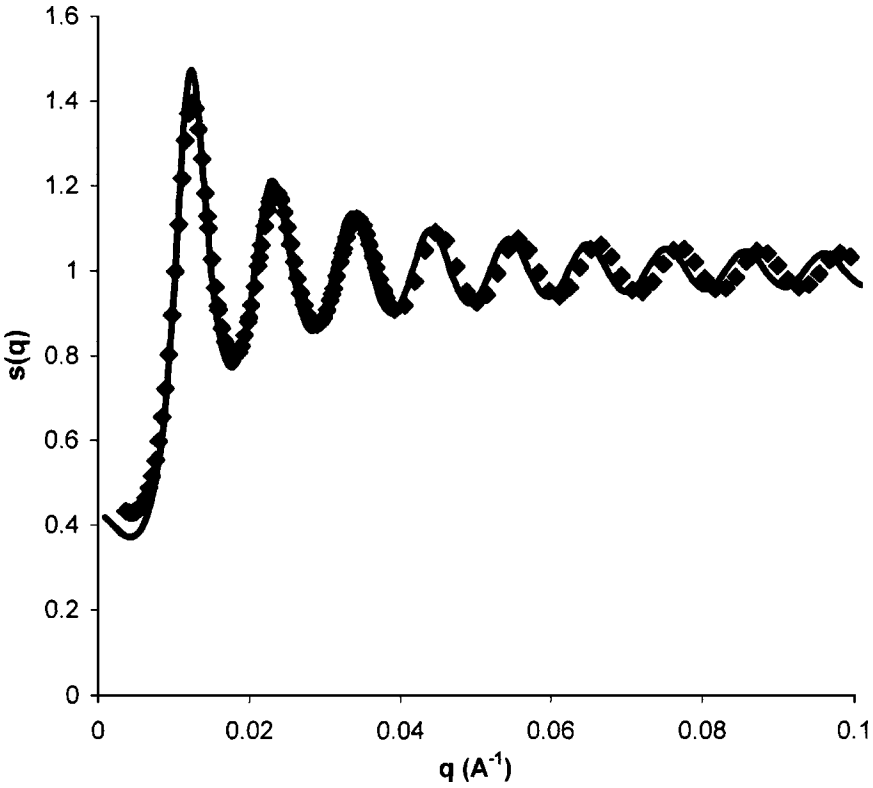

FIG. 3. Comparison of structure factor for the osmotic overlap model with depletion attractions [Eq. (28)] from the solution of the Percus-Yevick equation [Eqs. (15) and (16), solid line] compared with the model of Menon *et al.* (1991) [Eqs. (18)–(25)] using the effective hard-sphere diameter Eq. (30). Core diameter = 31 nm, corona thickness = 15.5 nm with 5000 Pa osmotic pressure in the layer and τ_b of 0.25.

$$D = \sigma + \int_0^{2L} \left(1 - \exp\left[-\frac{\pi\sigma}{kT}(\Delta\Pi^{\text{overlap}}_{\text{gelatin}})(L - H/2)^2\right]\right) dH, \tag{30}$$

where H is the surface to surface separation. The effective volume fraction is calculated from the effective diameter as $\phi_{\text{eff}} = \phi_{\text{core}}(D/\sigma)^3$.

This final conversion to a Baxter sticky hard-sphere model is performed to make rheological predictions and the corresponding square well for predictions of the SANS. The mapping is performed by equating second virial coefficients using Eqs. (10)–(12). As all of the parameters in the potential are independently measured, predictions of the zero-shear viscosity and SANS intensity can be directly compared against experiments without fitting parameters.

The structure factor for the full attractive potential could be directly calculated from Eqs. (15) and (16), thus avoiding the mapping to the square-well potential. However, the perturbative solution is accurate for the parameters under exploration here and is much more convenient mathematically. The accuracy of the perturbation solution is shown in Fig. 3 as a plot of the exact solution of the osmotic potential with attraction for monodisperse systems [calculated from Eqs. (15) and (16)] and the perturbative solution of Menon *et al.* [Eqs. (18)–(25)] for a core diameter = 31 nm, corona thickness = 15.5 nm, with 5000 Pa osmotic pressure in the layer, and $\tau_b = 0.25$ (these represent typical condi-

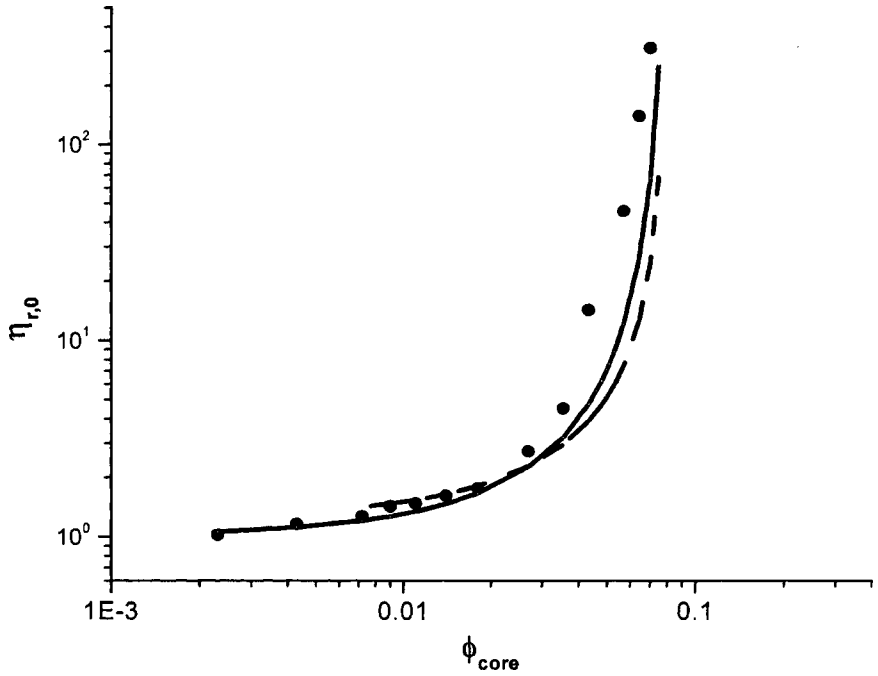

FIG. 4. Measured zero-shear relative viscosities for silica in gelatin vs model predictions at 40 °C, 10 mM salt, and *p*H 8 [Krishnamurty *et al.* (2004)]. The solid line is Eq. (2) and the dashed line Eq. (3), both with the effective hard sphere size determined from the osmotic overlap potential and Eq. (30). The uncertainty in data is of order of the symbol size.

tions for our system). As seen from Fig. 3, the simpler perturbation calculation agrees well with the exact calculation. Hence, this perturbative solution will be used for further analysis.

IV. RESULTS AND DISCUSSION

A. Effective hard-sphere modeling

The zero-shear viscosities of mixture of silica and gelatin at *p*H in 10 mM sodium acetate buffer at 40 °C are shown in Fig. 4. As shown previously, [Krishnamurthy *et al.* (2004)] a substantial Newtonian plateau is evident for all samples and the uncertainty in the measurements is on the order of the symbol size. It is readily apparent that the adsorbed gelatin greatly increases the effective hard-sphere volume fraction of the silica, as the zero-shear viscosity diverges around 10 vol % silica, while for hard spheres the divergence is around 58%. Note that the divergence is not due to bridging or other phenomena-as rheological measurements show a significant Newtonian plateau without measurable elasticity. SANS measurements—discussed next—confirm that the particles are stable and dispersed as individual particles.

Figure 4 also shows the predictions of a purely repulsive osmotic overlap potential using Eq. (28) with 5200 Pa osmotic pressure of gelatin in the adsorbed layer of thickness 15.5 nm, yielding an effective diameter of $D=59$ nm. The effective volume fraction is used in Eq. (2) with $\phi_{max}=0.58$ to predict the zero-shear viscosity. Notice that the correction for gelatin adsorption dominates the predictions (the ratio of $D/\sigma \sim 1.9$). The prediction of the correlation suggested for hard spheres by Cheng *et al.* (2002) demon-

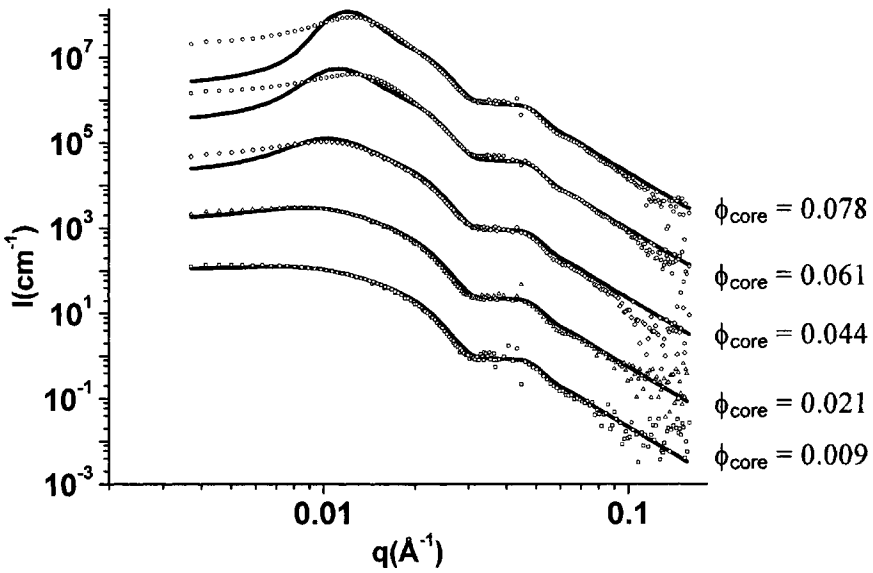

FIG. 5. Measured SANS for silica in gelatin vs model predictions at 40 °C, 10 mM salt, and *pH* 8. The solid line is the effective hard-sphere prediction. The intensities are shifted vertically for clarity.

strates poorer agreement. Thus, the systematic deviations with experiment for predictions based on an effective hard-sphere size are not a consequence of the choice of model for the hard-sphere viscosity. Furthermore, adjusting the maximum packing fraction ($\phi_{\max}$) cannot improve the comparison.

As shown, the osmotic overlap model *underpredicts* the zero-shear viscosities. The same trend is also observed for the Huggins coefficient. The hard-sphere limit for the Huggins coefficient is 0.946 [Bergenholtz and Wagner (1994)], while that measured for our gelatin-coated system is 5.8 ± 3 and that reported by Vaynberg and Wagner (2001) is 6 ± 2, which indicates the presence of additional interparticle interactions. As defined by Eq. (1), k_H will not be affected by the increased hydrodynamic diameter due to gelatin adsorption if the adsorption solely leads to an increased effective hard-sphere interaction. Note, however, that attractions as well as repulsions increase k_H above the hard-sphere value [Bergenholtz and Wagner (1994)], such that rheology alone will not be able to distinguish the nature of deviation from the hard-sphere behavior.

Figure 5 shows the results of SANS measurements for a series of silica volume fractions at the same gelatin concentration as the rheology tests (5 mg/ml free gelatin). The hard-sphere structure factor is calculated from Eqs. (15) and (16) (i.e., the Percus-Yevick-Ornstein-Zernike equation for hard spheres) using the effective hard-sphere diameter D calculated from Eq. (30). The measured scattering curves have been shifted vertically for clarity.

It can be seen from Fig. 5 that the effective hard-sphere model is able to predict the SANS measurements at low volume fractions of silica. However, at high volume fractions, the predicted scattering intensities are orders of magnitude lower than the measured intensities at small scattering vectors. The forward scattering is related to the osmotic compressibility of the dispersion [McQuarrie (2000)], such that the observed trends indicate that that the dispersion's osmotic pressure increases less rapidly with concentration than predicted by the effective hard-sphere model. Note that the particle polydispersity

and instrument smearing have been properly accounted for in comparing theory and experiments. Consequently, the discrepancy indicates systematic deviations from hard-sphere behavior.

Comparison of the effective hard-sphere model predictions to measurements of viscosity and microstructure clearly indicates systematic deviations. Further, corrections to the thermodynamic and rheological effective hard-sphere sizes must be in opposing directions to quantitatively match the data. This is not feasible within the framework of a simple repulsive interaction. However, the physical observations can be reconciled if *weakly attractive interparticle interactions* are present in the system. Weak attractions will increase the zero-shear viscosity but lower the osmotic pressure [and hence, increase the forward scattering $I(0)$]. The weak attractions are postulated to arise from depletion interactions due to the presence of free gelatin in the colloid—gelatin mixture, similar to the observations of Snowden *et al.* (1991). The Asakura—Oosawa potential is employed to make improved predictions of the dispersion rheology and equilibrium structure. For systems without the free polymer, attractions may also be a consequence of some inherent "stickiness" between adsorbed gelatin molecules on different particles (note that the gelatin temperature of gelatin $T_{gel} \sim 37\ ^\circ C$ for gelatin at these conditions).

B. Including depletion interactions

The following procedure is followed to predict the zero-shear viscosity and SANS measurements for the potential including osmotic overlap and depletion attractions:

(1) The effective hard-sphere diameter resulting from steric repulsion is calculated from the adsorbed amount and corona thickness using Eq. (30).
(2) The effective volume fraction is calculated by rescaling the colloid volume fraction with $(D/\sigma)^3$ to account for the excluded volume arising from the adsorbed gelatin.
(3) The depletion potential $U(r)$ is calculated using $\Delta = R_g$ and the free gelatin concentration in the medium to obtain $\Pi^{free}_{gelatin}$ [Eq. (28)].
(4) The second virial coefficient of the Asakura-Oosawa potential can be equated to the Baxter sticky hard-sphere model to determine τ_b [Eqs. (10) and (11)].
(5) The stickiness parameter and effective hard-sphere size are used to predict the zero-shear viscosity with the proposed model [Eq. (9)].
(6) The square-well potential parameter $U_0(\Delta = R_g)$ is calculated from matching the second virial coefficient to that of the Baxter potential. $S(q)$ is predicted using the SHSM model of Menon *et al.* [Eqs. (18)–(25)] and $I(q)$ from Eq. (27).

C. Effect of colloid concentration- fixed gelatin 5 mg/ml

The procedure outlined above can be used to predict the zero-shear viscosity of gelatin-stabilized colloids shown in Fig. 4. The potential parameters, e.g., the osmotic pressure of free gelatin and the radius of gyration of gelatin, are specified from previous studies. The osmotic data presented in our previous work [Krishnamurthy *et al.* (2004)] have been refit to get better correlation for the osmotic pressure of gelatin at low concentrations. The osmotic pressure is fit to the form

$$\Pi(x, pH) = Ax + BxpH + Cx^{2.25}, \tag{31}$$

where x is the mass fraction of gelatin. The fit parameters A, B, and C are tabulated in Table III. The osmotic pressure of free gelatin at the condition of interest (5 mg/ml, pH 8) is $\sim$200 Pa.

TABLE III. Osmotic pressure parameters [Eq. (31)] for gelatin.

Parameter	Value (Pa)
A	-4.21×10^{4}
B	9.86×10^{3}
C	-2.62×10^{6}

Vaynberg *et al.* (1998) measured the radius of gyration of gelatin $R_g=14\pm2$ nm using SANS at the conditions of interest. Equating the second virial coefficients from Eq. (10) and (11) gives a range of values for τ_b (0.088 for $R_g=14$ nm and 0.195 for $R_g=12$ nm) at the conditions of interest.

Figure 6 shows the predictions of Eq. (9) for the zero-shear viscosity of gelatin-silica system for $\tau_b=0.088$ and 0.135, which are substantial improvements over those of the effective hard-sphere model without attractions shown in Fig. 4. The quality of the prediction is excellent for τ_b of 0.135, which corresponds to the lower end of the reported value of R_g. Given the approximate form of the potential and the fact that the parameters that go into this prediction are independently measured, this agreement validates the approach presented here for calculating the zero-shear viscosity of the polyampholyte-stabilized colloids. Also, using the lower range for R_g of gelatin is qualitatively consistent with the predictions of more sophisticated theories for depletion attraction, such as PRISM, which predict a lower second virial coefficient in comparison to that of the Asakura

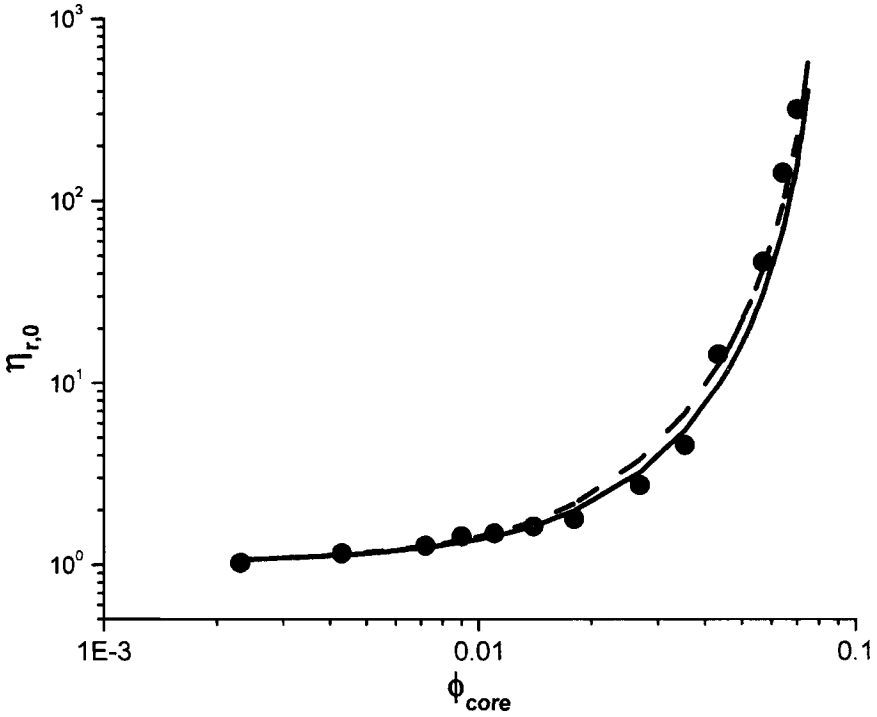

FIG. 6. Measured zero-sphere relative viscosities for silica in gelatin vs model fit at 40 °C, 10 mM salt, and *p*H 8. The dashed line is the prediction of Eq. (9) with $\tau_b=0.088$ ($R_g=14$ nm). The solid line is the prediction of Eq. (9) with $\tau_b=0.135$ ($R_g=12.5$ nm). The uncertainty in data is of order of the symbol size.

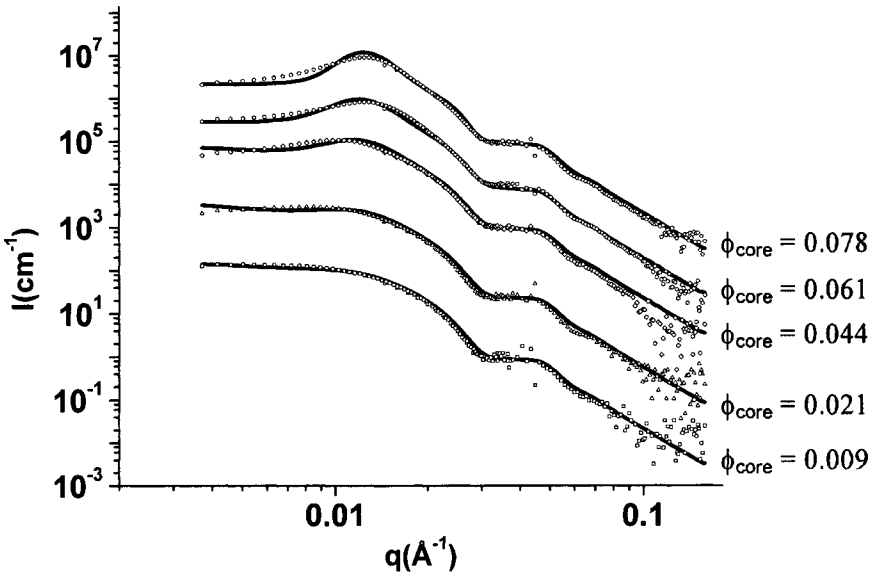

FIG. 7. Measured SANS for silica in gelatin vs model predictions at 40 °C, 10 mM salt, and *p*H 8. The solid line is the adhesive hard-sphere prediction. The parameters are tabulated in Table IV. The intensities are shifted vertically for clarity.

Oosawa model [Chatterjee and Schweizer (1998a, b)]. The Huggins coefficient can be calculated from Eq. (10) to be 4.39 (τ_b=0.088) to 3.19 (τ_b=0.135), which also compares well with the measured value of 5.8±3.

The value of τ_b that predicts the zero-shear viscosity (τ_b=0.135) can be independently verified by comparing *predictions* for the suspension microstructure with SANS measurements, as shown in Fig. 7. The scattering constant I_0 has been adjusted to within the uncertainty in the calculated values. The model parameters are tabulated in Table IV. As seen from Fig. 7, the prediction of the SANS measurements with the same independently measured parameters that predict the rheology is very good. This is a major improvement over what is predicted from the effective hard-sphere model as seen from Fig. 5 and earlier reports in the literature. Hence, we conclude that weak attractions must to be taken into account to completely describe this gelatin-stabilized colloidal dispersion.

TABLE IV. Parameters for SANS prediction in Fig. 7. The FWHM of neutrons is 14.7% and polydispersity is 8%. I_0 was calculated from parameters reported in Table II.

Volume fraction of silica	Free gelatin (mg/ml)	Calculated I_0 (cm^{-1})	I_0 for best fit (cm^{-1})	D_{core} (nm)	D_{eff} (nm)	τ_b
0.009	5	220	185	31	59	0.135
0.021	5	522	450	31	59	0.135
0.044	5	1061	1006	31	59	0.135
0.061	5	1434	1508	31	59	0.135
0.078	5	1760	1584	31	59	0.135

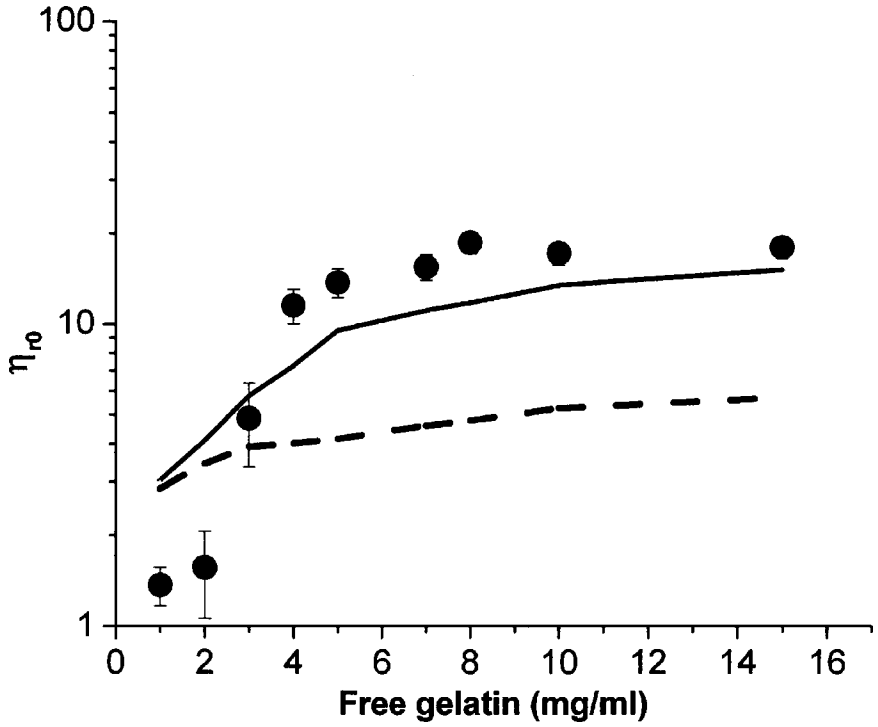

FIG. 8. Measured zero-shear relative viscosities for silica ($\phi_{core}=0.043$) in gelatin vs model at 40 °C, 10 mM salt, and *p*H 8. The dashed line is the prediction of Eq. (2) accounting for osmotic repulsion in the brush and the solid line is the prediction of the Eq. (9) accounting for additional depletion attractions., The parameters are tabulated in Table V.

D. Effect of gelatin concentration-fixed colloid volume fraction

To further test the proposed model, experiments were performed at a fixed silica volume fraction of 0.043 and varying background gelatin concentration. Figure 8 shows a plot of the measured relative zero-shear viscosities of these samples compared with the predictions. The relative viscosity shows an initial increase with increasing background gelatin, but plateaus at a gelatin concentration of about 5 mg/ml gelatin. A similar result was reported by Buscall *et al.* (1993), i.e., an initial increase in viscosity with increasing polymer concentration followed by a plateau when the concentration of the polymer in the background is in the semidilute region. This was attributed to the saturation in the depletion potential resulting from polymer chain overlap in the semidilute regime. The correlation length of the polymer, which determines the magnitude of depletion attraction, scales with R_g for a neutral polymer in the dilute region but scales as $R_g c^{-0.75}$ in the semidilute region. This leads to a saturation in $U(r)$ with increasing polymer concentration, which results in a plateau in the *relative* viscosity. This transition is observed at about 5 mg/ml, which is the value of c^* reported by Pezron *et al.* (1991) for similar gelatin solutions. Note that solutions of our gelatin at these conditions do not form a sample spanning gel below this gelatin concentration upon lowering the temperature below the gel point.

Figure 8 also shows the predictions of the effective hard-sphere model Eq. (2) with the osmotic overlap correction [Eq. (19)] as well as the model including attractions, Eq. (9). The interaction potential τ_b has been assumed to plateau at 5 mg/ml. Below this concen-

TABLE V. Parameters for predicting the data presented in Fig. 8. Silica volume fraction is 0.043. $R_g = 12$ nm.

Free gelatin (mg/ml)	Adsorbed gelatin (mg/m^2)	Osmotic pressure of free gelatin (Pa)	D_{eff} (nm)	τ_b
1	0.58	38	55	1.61
2	1.03	77	57	0.72
3	1.39	117	58	0.33
4	1.69	159	59	0.24
5	1.94	203	59	0.135
7	2.33	298	60	0.135
8	2.49	347	60	0.135
10	2.75	454	61	0.135
15	3.19	763	61	0.135

tration the potential is calculated from Eq. (28) with R_g of 12 nm and the osmotic pressure using Eq. (31). Again the predictions of the model accounting for both repulsive and attractive interactions yield a significant improvement over the effective hard-sphere model. The predictions are quantitative except at very low concentrations of gelatin, where possible incomplete coverage complicates the interpretation of the measurements. The parameters used are tabulated in Table V.

Figure 9 shows the SANS for a fixed silica volume fraction of 0.05 at different gelatin concentrations along with the predictions of the model including both repulsive and attractive interactions due to adsorbed and free gelatin, respectively. The SANS parameters are tabulated in Table VI. Again, there is excellent agreement between model predictions that include attractions and the measurements. Also shown are the dashed lines for the effective hard-sphere model. Clearly, accounting for the free gelatin is necessary to properly predict the measured dispersion microstructure.

E. Comparison to additional data from the literature

Hone *et al.* (2000) measured the shear viscosity of polystyrene latex stabilized by gelatin in aqueous solution at various conditions. They modeled the shear viscosity to estimate the adsorbed and free gelatin and the effective hard-sphere size due to adsorbed gelatin, and measured the hydrodynamic size of these complexes using DLS at some conditions. Interestingly, they extracted a greater *rheological layer thickness* compared to a *hydrodynamic layer thickness* obtained from DLS. This suggests the presence of weak attractions due to the presence of free gelatin in the dispersions.

Vaynberg and Wagner (2001) measured the zero-shear viscosity of aqueous acrylic latex dispersions stabilized by gelatin. Their experimental protocol differed slightly from that presented here as they removed the free gelatin by repeated centrifugation. Since there is no free gelatin in the system, the Asakura-Oosawa model predicts that the value of τ_b should be large (i.e., the system should be close to the hard-sphere limit). However, it is plausible that residual weak attractions may arise in these dispersions due to gelatin-gelatin interactions between the adsorbed layers, as the dispersions are only a few degrees above the gel transition ($\sim$37 °C). Alternatively, inherent van der Waals forces could also be a source of attractions.

The zero-shear viscosities from these published reports are plotted in Fig. 10. It was shown previously that these data could be largely reduced to a master curve by using an effective hard-sphere size accounting for the adsorbed gelatin [Krishnamurthy *et al.*

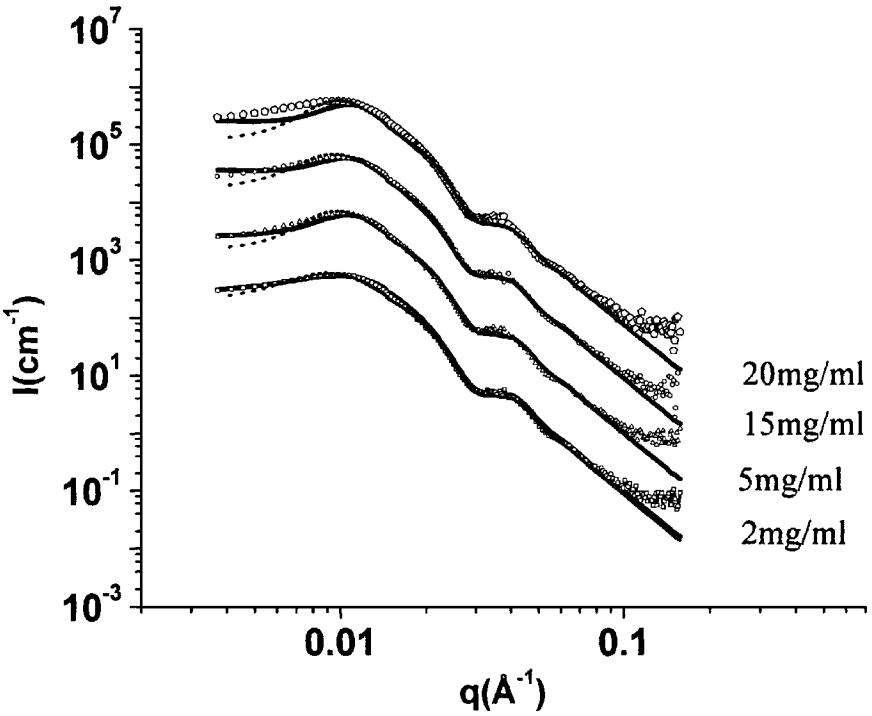

FIG. 9. Measured SANS for silica in gelatin vs model predictions at 40 °C, 10 mM salt, and *p*H 8. The gelatin concentration is varied as noted. The solid line is the adhesive hard-sphere prediction. The dashed line is the prediction of the effective hard-sphere model without attractions. The parameters are tabulated in Table VI. The intensities are shifted vertically for clarity.

(2004)]. Figure 11 shows a master plot suggested by Eq. (9); the relative viscosity for the systems in Fig. 10 is divided by the term $(1+1.9\phi^2/\tau_b)$ and plotted against the effective volume fraction. When plotted in this manner a master curve corresponding to η_{r0}^{HS} should result. The hydrodynamic size was used to estimate the effective particle size and the value of τ_b was fit and reported in Table VII. Two sets of data amenable to the analysis have been used from Hone *et al.* (2000): the 52 nm (diameter) rheology set with the reported corona thickness of ~38 nm in absence of electrolyte (Table 3b in the reference); 134 nm particles with no added salt (Table 4a in the reference) at constant gelatin concentration of 0.5%. The reported DLS diameter is about 43 nm and the relative viscosities presented in that paper are used directly for the analysis. Also shown are the two hard-sphere models [Eqs. (2) and (3)].

TABLE VI. Parameters for SANS prediction in Fig. 9.

Volume fraction of silica	Free gelatin (mg/ml)	Calculated I_0 (cm^{-1})	I_0 for best fit (cm^{-1})	D_{core} (nm)	D_{eff} (nm)	τ_b
0.052	2	1256	968	31	57	0.72
0.052	5	1232	1019	31	59	0.135
0.050	15	1128	1028	31	62	0.135
0.050	20	1107	985	31	63	0.135

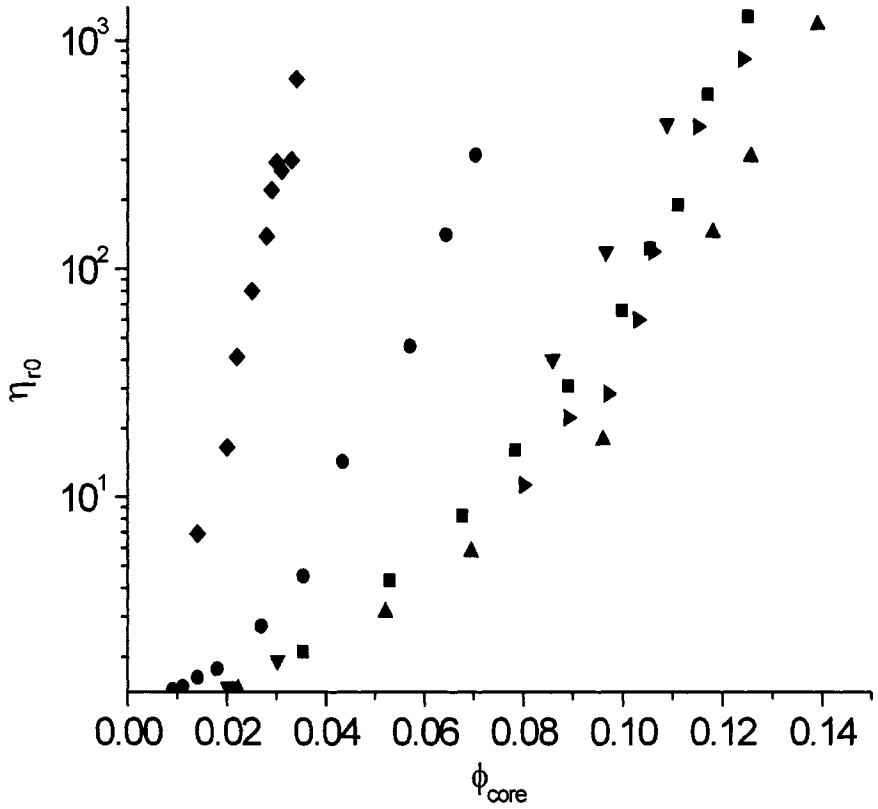

FIG. 10. Relative viscosity of gelatin coated particles at different *p*H/salt plotted as a function of the bare colloid concentration from Vaynberg and Wagner (2001) *p*H 5.8(▼), 6.5(■) and 8(▲), Hone *et al.* (2000) 26 nm PS on salt (♦) and 67 nm no salt in 0.5% gelatin (►) and this work (●).

Figure 11 demonstrates that a master curve for these complex systems can be achieved if both the excluded volume due to the adsorbed gelatin and weak attractions due to free gelatin and gelatin corona interactions are accounted for. As noted previously, there are deviations for some data sets at high packing fractions suggesting effects of polydispersity or possible adsorbed layer compression may be relevant near maximum packing.

The systems described so far have free-gelatin concentrations below or slightly above c^*. The concentration of free gelatin is small compared to the concentration in the adsorbed layer. Recent work [Hone and Howe (2002)] has shown that at very high gelatin concentrations (approximately 10× compared to this work), the dispersions show a qualitatively different rheological behavior; they show an exponential increase in viscosity as the colloid volume fraction increases. The effective volume fractions of the colloid approach 200% based on rescaling the diameter determined from DLS, suggesting substantial corona overlap. This observation can be reconciled to some extent by accounting for the potential arising from both the adsorbed and free gelatin within the framework proposed in this work. Vaynberg *et al.* (1998) reported a plateau adsorption of gelatin on latex of about 1.5 mg/m^2. From this, the adsorbed and free gelatin concentrations is calculated using a mass balance and the reported concentrations of silica and gelatin. Based on the reported hydrodynamic sizes, the concentration of gelatin in the free solution is calculated to be higher than that in the adsorbed corona. Thus, according to the simplified osmotic overlap model there will be no steric repulsion as $\Delta\Pi^{\text{overlap}}_{\text{gelatin}}$ is nega-

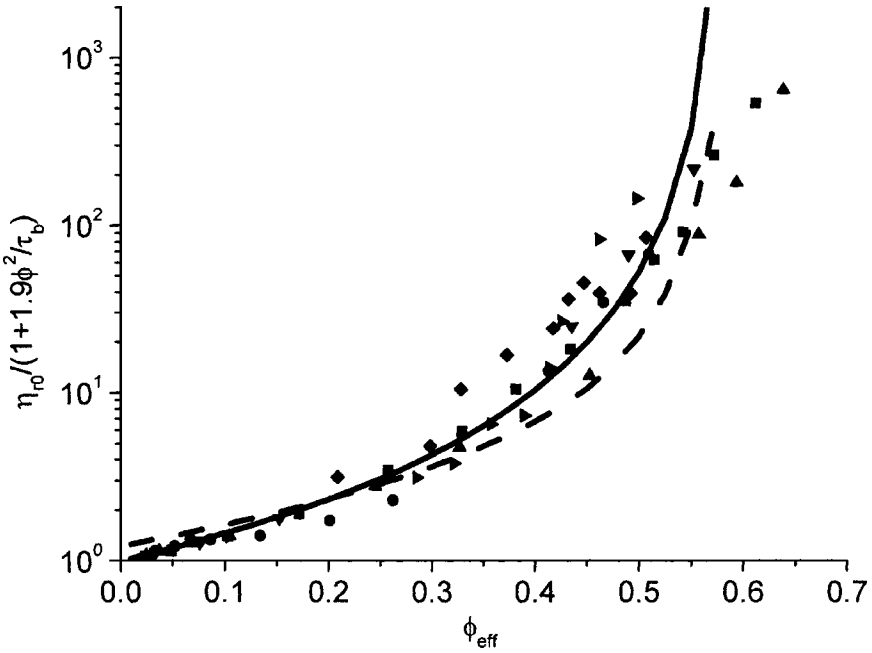

FIG. 11. Data rescaled with calculated volume fraction and corrected for attractions from Vaynberg and Wagner (2001) *p*H 5.8 (▼), 6.5(■) and 8(▲), Hone *et al.* (2000) 26 nm PS no salt(♦) and 67 nm PS no salt in 0.5% gelatin (►) and this work(●). The parameters are tabulated in Table VII. Also shown for reference are predictions of hard sphere equation Eq. (2) with $\phi_{max}=0.58$ (solid line) and Eq. (3) (dashed line).

tive. However, compression of adsorbed gelatin layer as two particles approach to $H<L$, will result in a further concentration of gelatin in the overlap volume, resulting in a steep steric repulsion [Fritz *et al.* (2002)]. Thus, the effective hard-sphere size should be on the order of $\sigma+L$. Estimates for the relative zero-shear viscosities are calculated by

TABLE VII. Rheological parameters for Fig. 11.

Source	Core radius (nm)	Corona thickness (nm)	*p*H	Salt (mM)	Adsorbed amount (mg/m^2)	D_{corr} (nm)	τ_b	τ_b (from calculation)
Vaynberg and Wagner (2001)	33	26	5.7	10	1.5	4.1	0.52	∞
Vaynberg and Wagner (2001)	33	27	6.6	10	1	4.6	0.59	∞
Vaynberg and Wagner (2001)	33	26.5	8.0	10	0.8	4.4	0.95	∞
Krishnamurthy *et al.* (2004)	15.5	15.5	8.0	10	4	2.5	0.135	0.08–0.195
Hone *et al.* (2000) (Table 3 in reference)	26	37	6.0	0	4.15	⋯	0.08	⋯
Hone *et al.* (2000) (Table 4 in reference)	67	43	6.5	0	2	⋯	0.12	⋯
Hone and Howe (2002)	57	11.5, 16.5 and 21 nm[a]	5.75	10	1.5	⋯	0.15	⋯

[a]One half of the reported thickness to account for significant layer compression.

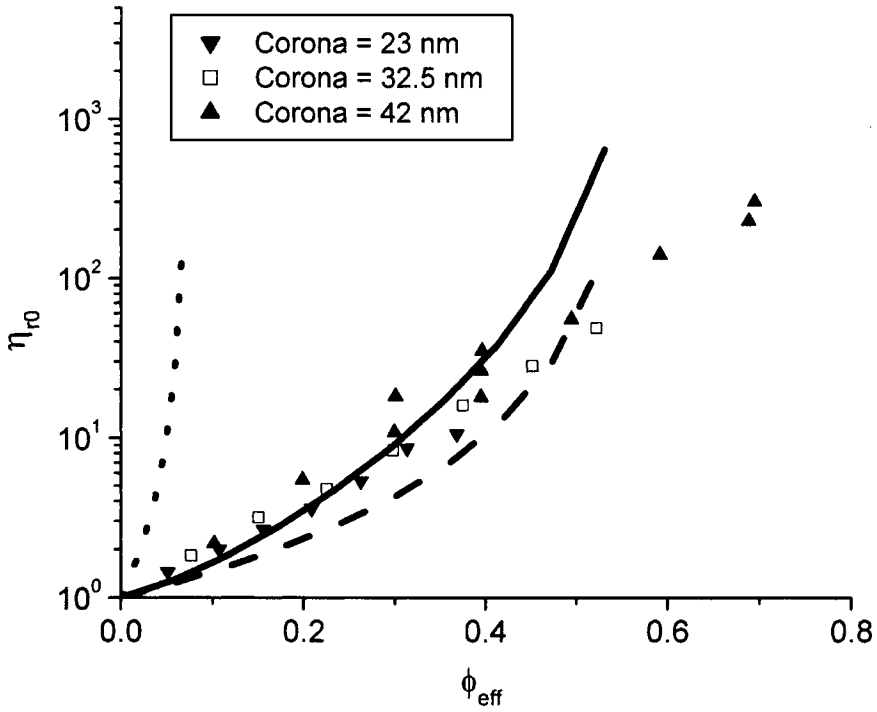

FIG. 12. Relative viscosity of gelatin coated particles for different gelatins plotted as a function of the effective colloid concentration from Hone and Howe (2002) Gel A with 23 nm corona thickness measured from DLS (▼), Gel B 32.5 nm corona (□) and Gel D with a 42 nm corona (▲). The bare particle was 57.1 nm in diameter. Data plotted with volume fraction rescaled with half the reported hydrodynamic layer thickness. The dotted line is the prediction of Eq. (2) with a hard-sphere size based on the reported DLS diameter for the 23 nm particle. Dashed line is the prediction of Eq. (2) and the solid line is the prediction of Eq. (9) with $\tau_b=0.15$, both accounting for brush overlap.

rescaling the volume fractions with $(\sigma+L/\sigma)^3$. Using $\tau_b=0.135$, which is expected to be approximate for these high gelatin concentrations, reasonable predictions can be realized until $\phi_{\text{eff}}\sim 0.4$ as can be seen from Fig. 12. The deviations at higher packing fractions are not unexpected within the framework of the osmotic overlap model and would require a more sophisticated treatment of the adsorbed and free gelatin.

The parameters for the predictions are reported in Table VII along with estimates from the Asakura–Oosawa potential and equating second virial coefficients. As expected, a systematic trend can be observed from the fit values of τ_b. For systems with free gelatin from both our work, from Hone *et al.* (2000) and Hone and Howe (2002) a value of about 0.14 describes the system adequately for $C\sim C^*$. For the systems without free gelatin [Vaynberg and Wagner (2001)], the value of τ_b is large (>0.5) indicating the low amount of *stickiness*, or near hard-sphere behavior. For reference, the gas liquid critical point for the Baxter potential is $(\phi^{\text{critical}},\tau_b^{\text{Critical}})\sim(0.1213,0.0976)$ [Menon *et al.* (1991)]. The extracted τ_b values for all these systems are well above τ_b^{Critical} indicating that all of the samples are in the single-phase region at the concentration of colloids investigated, which is consistent with observations.

V. CONCLUSIONS

Stable colloidal suspensions of silica in aqueous gelatin solutions can be modeled as colloidal dispersions of silica with an adsorbed layer of gelatin suspended in aqueous

solution with free gelatin. An effective colloidal interaction potential that accounts for the repulsion due to the adsorbed gelatin, as well as the attraction arising from free gelatin inducing a depletion interaction, are shown to predict both the low shear relative viscosity and microstructure of these dispersions.

In this work, we present a new semiempirical constitutive equation for the zero-shear viscosity of colloidal dispersions with weak attractions in terms of parameters that can be independently measured. This model can be used to predict trends in the zero-shear viscosity of colloidal systems in the presence of free and adsorbing polymer. The proposed interparticle potential reconciles apparent discrepancies between the suspension rheology and microstructure observed in our work and reported by others in the literature. The modeling is applied to provide a consistent quantitative description of a broad range of measurements of colloid-gelatin dispersion rheology from the literature with predicted or estimated parameters. Consequently, the methodology presented here is anticipated to apply to broader classes of colloidal dispersions with grafted and adsorbing polymer as well as surfactants; further exploration of this is underway.

ACKNOWLEDGMENTS

The authors acknowledge D. Boris and R. Koestner (Eastman Kodak, Rochester, N.Y.), A. Howe (Kodak, Harrow), W.B. Russel (Princeton University), and J. Mewis (K.U. Leuven) for useful discussions. The NIST, Gaithersburg, MD is acknowledged for providing facilities for neutron scattering experiments. Funding for the project was provided by Eastman Kodak and IFPRI. One of the authors (L.K.) acknowledges support from the University of Delaware graduate competitive fellowship.

References

Asakura, S., and F. Oosawa, "On interaction between two bodies immersed in a solution of macromolecules," J. Chem. Phys. **22**, 1255–1256 (1954).

Asakura, S., and F. Oosawa, "Interaction between particles suspended in solutions of macromolecules," J. Polym. Sci. **33**, 183–192 (1958).

Barker, J. A., and D. Henderson, "Perturbation theory and equation of state for fluids. II: A successful theory of liquids," J. Chem. Phys. **47**, 4714–4721 (1967a).

Barker, J. A., and D. Henderson, "Perturbation theory and equation of state for fluids: The square-well potential," J. Chem. Phys. **47**, 2856–2861 (1967b).

Batchelor, G. K., "The effect of Brownian motion on the bulk stress in a suspension of spherical particles," J. Fluid Mech. **83**, 97–117 (1977).

Batchelor, G. K., "Diffusion in a dilute polydisperse systems of interacting spheres," J. Fluid Mech. **131**, 155–175 (1983).

Baxter, R. J., "Percus-Yevick equation for hard spheres with surface adhesion," J. Chem. Phys. **49**, 2770–2774 (1968).

Bergenholtz, J., and N. J. Wagner, "The Huggins coefficient of a square-well fluid," Ind. Eng. Chem. Res. **33**, 2391–2397 (1994).

Brady, J. F., "The rheological behavior of concentration colloidal dispersions," J. Chem. Phys. **99**, 567–581 (1993).

Buscall, R., J. Ian McGowan, and A. J. Morton-Jones, "The rheology of concentrated dispersions of weakly attracting colloidal particles with and without wall slip," J. Rheol. **37**, 621–641 (1993).

Chatterjee, A. P., and K. S. Schweizer, "Correlation effects in dilute particle-polymer mixtures," J. Chem. Phys. **109**, 10477–10489 (1998a).

Chatterjee, A. P., and K. S. Schweizer, "Microscopic theory of polymer-mediated interactions between spherical particles," J. Chem. Phys. **109**, 10464–10476 (1998b).

Cheng, Z., J. X. Zhu, P. M. Chaikin, S. E. Phan, and W. B. Russel, "Nature of divergence in low shear viscosity of colloidal hard sphere dispersions," Phys. Rev. E **65**, 041405-1–041405-8 (2002).

Cichocki, B., and B. U. Felderhof, "Diffusion coefficients and effective viscosity of suspensions of sticky hard spheres with hydrodynamic interactions," J. Chem. Phys. **93**, 4427–4432 (1990).

Cosgrove, T., J. H. E. Hone, A. M. Howe, and R. Heenan, "A small-angle neutron scattering study of the structure of gelatin at the surface of polystyrene latex particles," Langmuir **14**, 5376–5382 (1998).

Dawson, K., G. Foffi, M. Fuchs, W. Gotze, F. Sciortino, M. Sperl, P. Tartaglia, T. Voigtmann, and E. Zaccarelli, "Higher-order glass-transition singularities in colloidal systems with attractive interactions," Phys. Rev. E **63**, 011401–17 (2001).

Einstein, A., "On the theory of Brownian movement," *Investigations on the Theory of Brownian Movement*, edited by R. Furth (Dover, New York, 1956). Translation of papers appearing in Ann. Phys. **19**, 371–381 (1906); Ann. Phys. **34**, 591–592 (1911).

Eck, D., C. A. Helm, N. J. Wagner, and K. A. Vaynberg, "Plasmon resonance measurements of the adsorption and adsorption kinetics of a biopolymer onto gold nanocolloids," Langmuir **17**, 957–960 (2001).

Fritz, G., V. Schadler, and N. Willenbacher, "Electrosteric stabilization of colloidal dispersions," Langmuir **18**, 6381–6390 (2002).

Gast, A. P., C. K. Hall, and W. B. Russel, "Polymer-induced phase separations in non-aqueous colloidal suspensions," J. Colloid Interface Sci. **96**, 251–267 (1983).

Hansen, J. P., and I. R. McDonald, *Theory of Simple Liquids* (Academic, New York, 1986).

Hiemenz, P. C., and R. Rajagopalan, *Principles of Colloid and Surface Chemistry* (Marcel Dekker, New York, 1997).

Howe, A. M., "Some aspects of colloids in photography," Curr. Opin. Colloid Interface Sci. **5**, 288–300 (2000).

Hone, J. H. E., A. M. Howe, and T. H. Whitesides, "Rheology of polystyrene latexes with adsorbed and free gelatin," Colloids Surf., A **161**, 283–306 (2000).

Hone, J., and A. M. Howe, "Viscosity of colloidal suspensions in aqueous gelatin," J. Colloid Interface Sci. **251**, 193–199 (2002).

Kamiyama, Y., and J. Israelachvili, "Effect of pH and salt on the adsorption and interactions of an amphoteric polyelectrolyte," Macromolecules **25**, 5081–5088 (1992).

Kotlarchyk, M., and S. Chen, "Analysis of small angle neutron scattering spectra from polydisperse interacting colloids," J. Chem. Phys. **79**, 2461–2469 (1983).

Krieger, I. M., and T. J. Dougherty, "A mechanism of non-Newtonian flow in suspensions of rigid spheres," Trans. Soc. Rheol. **3**, 137–152 (1959).

Krishnamurthy, L. N., E. C. Weigert, D. C. Boris, and N. J. Wagner, "The shear viscosity of polyampholyte (gelatin) stabilized colloidal dispersions," J. Colloid Interface Sci. **280**, 264–275 (2004).

Likos, C. N., K. A. Vaynberg, H. Lowen, and N. J. Wagner, "Colloidal stabilization by adsorbed gelatin," Langmuir **16**, 4100–4108 (2000).

Lionberger, R. A., and W. B. Russel, "Microscopic theories of the rheology of stable colloidal dispersions," Adv. Chem. Phys. **111**, 399–474 (2000).

McQuarrie, D. A., *Statistical Mechanics* (University Science Books, Sausalito, CA, 2000).

Menon, S. V. G., C. Manohar, and K. Srinivasa Rao, "A new interpretation of the sticky hard sphere model," J. Chem. Phys. **95**, 9186–9190 (1991).

Mewis, J., and J. Vermant, "Rheology of sterically stabilized dispersions and lattices," Prog. Org. Coat. **40**, 111–117 (2000).

Pezron, I., M. Djabourov, and J. Leblond, "Conformation of gelatin chains in aqueous solutions. I. A light and small-angle neutron scattering study," Polymer **32**, 3201–3210 (1991).

Quemada, D., "Rheology of concentrated disperse systems and minimum energy dissipation principle. I: Viscosity concentration relationship," Rheol. Acta **16**, 82–94 (1977).

Rueb, C. J., and C. F. Zukoski, "Rheology of suspensions of weakly attractive particles: Approach to gelatin," J. Rheol. **42**, 1451–1476 (1998).

Russel, W. B., "Huggins coefficient as a means of characterizing suspended particles," J. Chem. Soc., Faraday Trans. 2 **80**, 31–41 (1984).

Russel, W. B., D. A. Saville, and W. R. Schowalter, *Colloidal Dispersions* (Cambridge University Press, Cambridge, UK, 1989).

Smith, N. J., and P. A. Williams, "Depletion floccuplation of polystyrene lattices by water soluble polymers," J. Chem. Soc., Faraday Trans. **91**, 1483–1489 (1995).

Snowden, M. J., C. M. Clegg, P. A. Williams, and I. D. Robb, "Flocculation of silica particles by adsorbing and non-adsorbing polymers," J. Chem. Soc., Faraday Trans. **87**, 2201–2207 (1991).

Vaynberg, K. A., N. J. Wagner, R. Sharma, and P. Martic, "Structure and extent of adsorbed gelatin on acrylic latex and polystyrene colloidal particles," J. Colloid Interface Sci. **205**, 131–140 (1998).

Vaynberg, K. A., and N. J. Wagner, "Rheology of polyampholyte (gelatin)-stabilized colloidal dispersions: The tertiary electroviscous effects," J. Rheol. **45**, 451–466 (2001).

Woutersen, A. J. T. M., and C. G. De Kruif, "The rheology of adhesive hard sphere dispersions," J. Chem. Phys. **94**, 5739–5750 (1991).